coatings

MDPI

Article

Enhancing Hydrophobic Properties in Olive Oil-Coated Papers through Thermal Treatment

Amelia Loesch-Zhang [1], Tobias Meckel [1], Markus Biesalski [1] and Andreas Geissler [1,2,*]

[1] Macromolecular and Paper Chemistry, Technical University Darmstadt, Peter-Grünberg-Str. 8, 64287 Darmstadt, Germany; amelia.loesch-zhang@tu-darmstadt.de (A.L.-Z.); tobias.meckel@tu-darmstadt.de (T.M.); markus.biesalski@tu-darmstadt.de (M.B.)
[2] Papiertechnische Stiftung (PTS), Pirnaer Str. 37, 01809 Heidenau, Germany
* Correspondence: andreas.geissler@tu-darmstadt.de

Abstract: Enhancing paper hydrophobicity is of key importance for many paper-based applications. Fatty acids or vegetable oils and their derivatives replace environmentally harmful conventional coating materials but still require challenging chemical reactions for covalent attachment onto paper. Here, we show that simple storage of olive oil-coated cotton linter paper at 70 °C and subsequent Soxhlet extraction is able to endow paper with hydrophobic properties, reaching water contact angles above 130°. In-depth chemical and morphological analytics show the relevance of temperature and air accessibility during the aging process compared with aging at ambient temperature and under the exclusion of oxygen, underlining the importance of assessing a coating's long-term performance and stability under diverse storage conditions. Simple storage of vegetable oil-coated paper at elevated temperatures followed by extraction proves to be an easy way to produce stable covalently attached hydrophobic paper coatings with exceptionally low coating amounts.

Keywords: aging; dip coating; hydrophobicity; olive oil; paper; water contact angle

Citation: Loesch-Zhang, A.; Meckel, T.; Biesalski, M.; Geissler, A. Enhancing Hydrophobic Properties in Olive Oil-Coated Papers through Thermal Treatment. *Coatings* **2024**, *14*, 364. https://doi.org/10.3390/coatings14030364

Academic Editor: Fábio Ferreira

Received: 12 February 2024
Revised: 8 March 2024
Accepted: 16 March 2024
Published: 20 March 2024

1. Introduction

In view of the global challenge to reduce consumption of fossil-based resources, plant-based materials have shifted into focus, e.g., for the application of (super)hydrophobic paper coatings. (Super)hydrophobic coatings are required in manifold applications such as packaging, biosensing, textiles and membranes. As such, fatty acids and plant-based oils have shown great potential for improving surface hydrophobicity [1]. Fatty acid-derivative-based hydrophobization approaches for cellulosic materials include esterification reactions based on fatty acyl chlorides such as stearoyl chloride, oleoyl chloride and palmitoyl chloride [2–4], which even give access to superhydrophobic coatings [5–7]. Transesterification can also be performed under supercritical solvent conditions, e.g., using sunflower oil [8]. Further approaches include grafting processes such as ring-opening polymerization [9], crosslinking processes [10–12], plasma polymerization [13] or application as part of hybrid organic nanoparticles [14] using a large variety of oils such as derivatives of soybean, castor, chia oil and olive oil. A simple process of immersing cotton substrates in organic solutions of soybean oil and subsequent heating to 120 °C for 1 h followed by acetone rinsing imparted water contact angles (WCAs) of up to 80°, while fully hydrophobic properties could not be achieved despite the use of a rather rough substrate [15].

In consideration of their importance in food industry, the aging process of fatty acids and vegetable oils has been extensively examined [16–22]. It is well known that vegetable oils undergo oxidation and hydrolysis processes during storage and that air accessibility, light exposure and high temperature accelerate this process [16–18]. Oxidation processes are induced by radical mechanisms wherein initially, a hydrogen radical is abstracted from the vicinity of a C=C double bond [23,24]. Concurrently, hydrolysis leads to the liberation of free fatty acids that in turn autocatalyze hydrolytic reactions [23–25]. Aging processes in paper

equally have been extensively examined and reviewed [26], but the work focused on the aging of the fibers rather than the coatings. To the best of our knowledge, the only research conducted on the aging of paper in combination with vegetable oils so far has focused on cellulosic materials used as insulators in transformers [24,27–30]. In this context, cellulosic materials, such as pressboard immersed in vegetable oil, were found to depolymerize during aging due to the presence and liberation of water, as indicated by an increase in 2-furfuraldehyde content [23,24,31]. The vegetable oil showed hydrolysis, oxidation and oxidative polymerization processes, resulting in increased viscosity and increased acid number that can, among others, be attributed to ester scission and polymerization [23,30]. Finally, a transesterification reaction occurs, in which free fatty acids formed as hydrolysis products react with cellulosic hydroxyl groups to form covalent ester bonds [24,29,32].

Not only the processes required to produce (super)hydrophobic paper coatings are still relatively complicated, but especially, the modifications occurring in coatings subjected to thermal stress or aging processes are still poorly understood—despite their relevance with respect to long-term performance and stability. In this work, we show that it is possible to obtain hydrophobic coatings with WCAs above 130° through the simple process of thermal storage of olive oil-coated paper followed by Soxhlet extraction. To elucidate the underlying mechanisms, we further examine aging processes at norm climate and under argon for comparison using chemical and surface analytics.

2. Materials and Methods

2.1. Materials

Olive oil was purchased from Oehlmuehle Solling (Boffzen, Germany) and determined to contain 77% oleic acid, 13% palmitic acid and 5% linoleic acid as well as some minor component fatty acids by GC-MS/FID (for the procedure, see Supplementary Information). Acetone and ethanol (analytical grade) were purchased from Merck (Darmstadt, Germany), Fluorescent Brightener 28 (Calcofluor White) from Sigma-Aldrich (St. Louis, MO, USA), Sudan III powder (dye content ≥75%) from Carl Roth (Karlsruhe, Germany) and Sudan III staining solution (2.5 g/L in ethanol (99.0%, denatured)) from Morphisto (Offenbach, Germany). Argon (99.999%) was obtained from Westfalen (Muenster, Germany).

2.2. Methods

- Cotton linter handsheet production

Cotton linter laboratory handsheets (100 g/m^2) were produced from aqueous cotton linter dispersion (2.2 wt%, diluted to 0.16 wt%) after stirring for 30 min to avoid fiber entanglement. Sheets were formed on a Haage sheet-former BBS (Haage, Preissenberg, Germany) in accordance with ISO 5269-2 [33]. The sheets were dried under reduced pressure (93 °C, 10 min), and sheet grammage was determined by bone-dried paper weight. To allow for the papers to reach equilibrium water content, the sheets were stored at norm climate conditions (23 °C, 50% relative humidity) for 24 h before use.

- Coating preparation and aging

Cotton linter handsheets were cut into stripes of 7.5 × 2.5 cm and dip-coated with olive oil on a custom-built device at a withdrawal speed of 2 mm/s.

For aging experiments performed at norm climate, samples were stored in an open Petri dish under controlled climate (23 °C, 50% relative humidity). For thermal aging, samples were stored in an open petri dish at 70 °C in a Heraeus function line T12 incubator (Heraeus, Hanau, Germany). For aging under argon, samples were stored in Schlenk vials from which air was removed by triple application of vacuum to 10^{-3} mbar followed by argon purging. The storage time was 4 weeks unless stated otherwise.

Soxhlet extractions were performed with acetone (300 mL) for 6 h.

- Staining with Calcofluor White and Sudan III

To examine the coating penetration into the paper during aging using confocal laser scanning microscopy (CLSM), the cotton linter papers were first immersed into an aqueous

Calcofluor White solution (100 µM, 15 min), after which excess dye was removed by gentle shaking in distilled H_2O (15 min). The stained papers were dried under reduced pressure at (40 °C, 1.5 h). The papers were then dip-coated with olive oil, which was mixed with Sudan III (25 µg/g oil) for staining.

For the fluorescence imaging of the extracted papers, Calcofluor White staining was performed as described. For Sudan III staining, the papers were first immersed in ethanol (10 s) and then immersed in an alcoholic Sudan III solution (10 vol% in ethanol, 5 min), after which excess dye was removed by gentle stirring in ethanol (3×, 15 min). The stained papers were dried under reduced pressure (40 °C, 1.5 h). Reference papers were equally extracted prior to staining.

- Attenuated total reflectance–Fourier transformation infrared (ATR-FTIR) spectroscopy

ATR-FTIR spectra were recorded with a Spectrum 3 spectrometer (PerkinElmer, Waltham, MA, USA) between 4000 cm^{-1} and 650 cm^{-1} at a nominal resolution of 4 cm^{-1} and 10 scans directly on the paper substrate. Background correction was performed using Spectrum software (Version 10.7.2).

- Confocal laser scanning microscopy (CLSM)

CLSM images were taken on a Leica TCS SP8 microscope (Leica Microsystems, Mannheim, Germany) with an HC PL APO CS2 20×/0.75 DRY objective. The samples were fixed in the sample holder without the use of coverslips and marked to reproduce the measurement position before and after aging. CFW fluorescence was excited at 405 nm, and emission was detected between 424 nm and 496 nm. Sudan III fluorescence was excited in a separate channel at 552 nm, and emission was detected between 561 nm and 681 nm. At each marked position, 3D image stacks were recorded with a plane-to-plane distance of 2 µm to capture the entire depth of said position. For presentation, maximum intensity projections were generated from the 3D stacks using ImageJ2 (Version 1.54b) [34].

- Differential scanning calorimetry (DSC)

DSC curves were measured both on coated paper and extracted oils using a Mettler Toledo DSC 3 calorimeter (Mettler Toledo, Gießen, Germany), and the data was evaluated using STARe software (Version 16.30a). Two cooling and heating cycles from 25 °C to −90 °C, and vice versa, were carried out at a cooling and heating rate of 5 K/min under nitrogen atmosphere (30 mL/min). The second cooling cycle was used for data evaluation. Crystallization enthalpies were determined for olive oil extracted from paper from the integral between −60 °C and −10 °C (5 °C for the thermally aged sample).

- Fluorescence imaging

Fluorescence images were recorded on a Vilber Fusion FX7 Edge Imager (Vilber, Eberhardzell, Germany) using (365 ± 20) nm and (530 ± 20) nm illumination combined with UV and orange emission filters, respectively. Due to its low depth discrimination (in contrast to CLSM imaging), this device is well suited to compare the emission intensities between samples.

- ^{1}H-Nuclear magnetic resonance (NMR) spectroscopy

NMR spectra were measured on a Bruker Avance II NMR spectrometer at 300 MHz, (Bruker BioSpin GmbH, Rheinstetten, Germany) in deuterated chloroform. Chemical shifts were calibrated to the deuterated solvent signal. MestReNova 11.0 software (Mestrelab Research S. L., Santiago de Compostela, Spain) was used to process the spectra.

- Optical profilometry

Surface roughness data was obtained by optical profilometry using a Sensofar PLu neox optical profiler (Sensofar-Tech, Terrassa, Spain) equipped with a Nikon EPI 20× objective ((850.08 × 709.35) µm scan area, 0.69 µm/pixel) using a 140 µm z-scan range. Measurements were repeated in triplicate, and surface roughness parameters S_a, S_q and S_z

were determined according to ISO 25178 [35]. Errors were calculated based on the standard deviation of the mean.

- Size exclusion chromatography (SEC)

Size exclusion chromatography (SEC) was performed using an Agilent Technologies system (Agilent Technologies, Santa Clara, CA, USA) equipped with an Agilent Technologies 1260 Infinity II G7129A autosampler, an Agilent Technologies 1260 Infinity II G7110B pump, an Agilent Technologies 1260 Infinity G1362A RI detector and a HP 1050 series UV detector and a PSS SDV 5 µm column. THF was used as a mobile phase at a flow rate of 1 mL/min and with an analyte concentration of (1.5–2) g/L.

- Water contact angle measurement

The coated papers were stored at norm climate conditions overnight before water contact angle measurements. Contact angles were measured on a Dataphysics OCA35 device (Dataphysics, Filderstadt, Germany) at norm climate conditions using the sessile drop method with 2 µL droplets of ultrapure water. Drop shape fittings were performed using Dataphysics SCA20 software and applying the Young–Laplace fitting mode. Individual data points were based on five different measurements, while time-dependent measurement series were repeated in triplicate. Advancing and receding contact angles were calculated as mean values of water contact angles measured during an increase of a 2 µL droplet by 10 µL at a speed of 1 µL/s and the subsequent decrease in that same droplet with the same parameters, also performed in triplicate. Errors were calculated from the standard deviation of the mean.

3. Results

In this work, we applied olive oil onto cotton linter laboratory handsheets via dip-coating and stored them for 4 weeks at either 70 °C, under norm climate (23 °C, 50% relative humidity) or at room temperature under argon (Figure 1). Afterward, excess oil was removed by Soxhlet extraction. Both the coated and extracted papers as well as the extracted oils were analyzed.

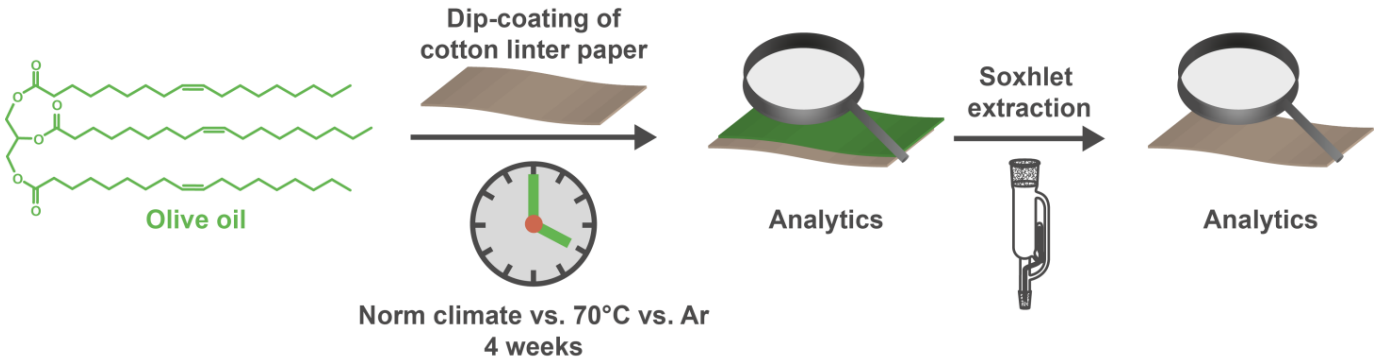

Figure 1. The approach used to examine the aging processes with olive oil as a coating material. Coated papers were stored for 4 weeks at norm climate, at 70 °C or under argon.

The olive oil-coated paper aged at 70 °C for 4 weeks shows a significantly enhanced water contact angle (WCA) of (97.4 ± 1.6)° compared with (66.0 ± 0.7)° for coated surfaces measured the day after coating. Soxhlet extraction leads to an even higher static water contact angle of (137.7 ± 1.2)°, which is stable for at least 5 min (Figure 2a), as well as advancing and receding WCAs of (137.9 ± 6.4)° and (122.9 ± 23.8)°, respectively. This is a strong indication that olive oil has in some way been covalently attached to the paper surface. Contrastingly, both the uncoated cotton linter paper and freshly coated paper submitted to subsequent Soxhlet extraction absorb water immediately, so WCA measurement is not possible. While the possibly covalently attached coating amount is too low to be detected in differential scanning calorimetry (DSC) measurements, attenuated

total reflectance–Fourier transformation infrared (ATR-FTIR) spectroscopy shows a weak signal at 1736 cm^{-1} that is not present in the cotton linter paper or in the freshly olive oil-coated extracted paper (Figure 2b, full spectrum in Figure S1). This band is indicative of C=O ester bonds [36] and indicates that transesterification has taken place, covalently linking a fatty acid chain of the oil to the cellulose hydroxyl groups, as has previously been observed [24,29,32]. Due to an overlap of the CH_2 vibration modes of fatty acids and cellulose in the region between 3000 cm^{-1} and 2800 cm^{-1} [36], this area cannot be taken into consideration for the current discussion. The low intensity of the characteristic olive oil bands compared with the cellulosic bands shows that the retained coating amount is very low. Furthermore, both the olive oil-coated and uncoated cotton linter papers were stained with Calcofluor White, a fluorescent dye that has a high affinity for cellulose, and Sudan III, a fat-soluble staining agent. Fluorescent imaging of the stained papers and an unstained reference proves the presence of fat in the aged paper after Soxhlet extraction, as Sudan III excitation yields much brighter images for the coated paper than for those not supposed to contain aliphatic species (Figure 2c). Notably, Calcofluor White emission is lower in the presence of either olive oil or Sudan III than without the hydrophobic coating.

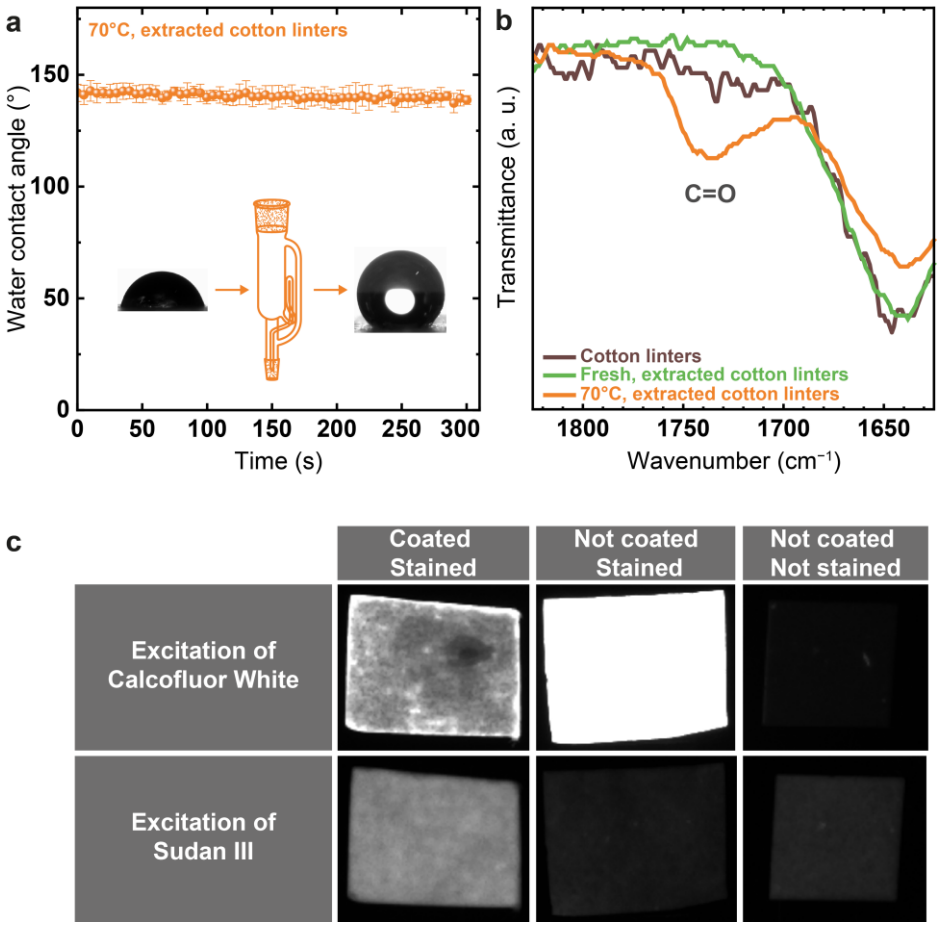

Figure 2. (**a**) WCA evolution for extracted thermally aged cotton linter paper over 5 min showing permanent hydrophobization. (**b**) Excerpt of FTIR spectra from 1625 cm^{-1} to 1825 cm^{-1} measured on extracted cotton linters after varying aging processes and showing a small C=O band indicating esterification exclusively after thermal aging. (**c**) Fluorescence images comparing coated stained, uncoated stained and uncoated unstained papers exciting either Calcofluor White or Sudan III. While CFW is observed in both stained samples, Sudan III is only present in the coated ones, proving the presence of fatty acids. All images of one channel were taken simultaneously and cropped for better display without further modification, original size of approximately (7 × 10) mm.

While these observations are convincing proof that transesterification leading to the covalent attachment of fatty acids onto cellulose occurs when paper ages at 70 °C, further inquiries into the aging process would deepen the understanding thereof and accordingly help to explain the increase in the WCA after thermal aging and Soxhlet extraction. As it is well known that both temperature and oxygen accessibility influence the aging of olive oil, we compared the aging processes occurring at 70 °C to those occurring during storage at norm climate and under argon.

Initially, we compared surface properties for the three aging processes. The water contact angles increase under all aging conditions, from (66 ± 0.7)° for the fresh sample to (77.8 ± 0.6)° after aging under argon atmosphere and to (82.9 ± 1.4)° after aging at norm climate, even to the aforementioned hydrophobic range with (97.4 ± 1.6)° after aging at 70 °C (Figure 3a). Complete water droplet absorption into the paper is slowed down compared with the uncoated paper and takes place within 15 s after deposition for the fresh and argon-aged samples, within 30 s for the samples aged at norm climate and around 4 min for samples aged at 70 °C (Figure 3b). Surface roughness measurements show no significant change in roughness parameters independent of the aging conditions, indicating that the water contact angle modification is not caused by a change in the wetting regime. Instead, the paper roughness is defined by the roughness of the cotton linter paper substrate and is not significantly modified by the vegetable oil coating (Figure 3c).

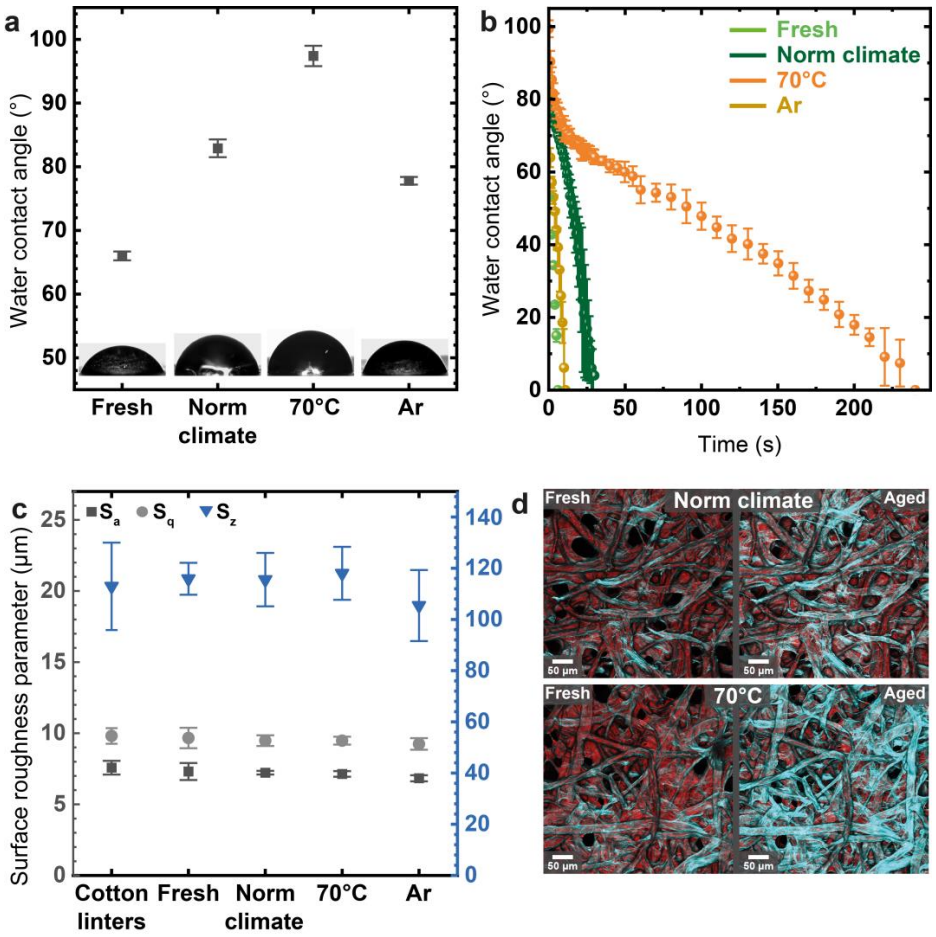

Figure 3. (**a**) Static and (**b**) time-dependent static WCA measurements showing increasing WCAs with air accessibility and temperature. (**c**) Surface roughness parameters show no significant modification with aging. (**d**) CLSM images showing the comparison between fresh and aged samples indicating a migration of oil from the fiber surface into the fiber wall, especially at 70 °C (cellulose stain in cyan, oil stain in red). Images were recorded with the same settings for excitation and emission (power and detector gain) and at the same position between fresh and aged samples.

The same fluorescent dyes for cellulose and oil, which were used above for fluorescent intensity imaging, were also used for confocal microscopic examinations. Images were taken at the very same positions on each paper sample before and after aging. The comparison between these time points reveals a marked increase in the Calcofluor White fluorescence intensity after storage (Figure 3d). An increased intensity of the Calcofluor White fluorescence in the absence of a Sudan III-stained oil coating was similarly observed in the aforementioned analysis with the fluorescent imager (Figure 2c). It is therefore reasonable to assume that the proximity of the coating and Calcofluor White on the fiber surface right after staining and dip coating—and before aging—causes the latter dye to fluoresce less. More importantly, the increase during aging then strongly points to a separation between Calcofluor White and the coating. This separation could be the result of a progressing migration of the oil from the fiber surface into the fiber wall. The observation that the increase in Calcofluor White fluorescence intensity is even stronger for paper aged at 70 °C supports this migration hypothesis, as temperature decreases the oil's viscosity, which facilitates migration.

Chemical analytics show the processes occurring within the coating during aging. To perform ^{1}H-nuclear magnetic resonance (NMR) spectroscopy and size exclusion chromatography (SEC), unbound coating material was extracted from the paper through Soxhlet extraction, and the oil residue obtained after solvent removal was analyzed. When performing ATR-FTIR spectroscopy and differential scanning calorimetry, both the coated paper and the extracted oil were examined, and the results were in good agreement with each other. The data shown is that of the coated paper.

^{1}H-NMR spectroscopy shows strong modifications for the samples stored at 70 °C. Integrals of all peaks indicating hydrogens in vicinity to double bonds decrease, namely, those at (5.50–5.30) ppm (R-C**H**=CH, decrease to ~2% of its original value), (2.10–1.93) ppm (C**H**$_2$-CH=CH, decrease to ~4% of its original value) and (2.85–2.70) ppm (CH=CH-C**H**$_2$-CH=CH, complete disappearance). Simultaneously, the integral of the peak indicating aliphatic chains at (1.45–1.15) ppm increases, as do all peaks indicating hydrogen groups in the vicinity of oxygen-containing groups, namely, those at (5.30–5.20) ppm (C**H**-O-CO-R), (4.35–4.10) ppm (C**H**$_2$-O-CO-R), (2.40–2.25) ppm (C**H**$_2$-CO-O-R/H) and (1.70–1.15) ppm (C**H**$_2$-CH$_2$-CO-O-R/H). Peak attribution was in good accordance with the literature [37]. These changes indicate that oxidative processes take place during thermal aging. For the coatings aged at norm climate, similar changes are observed, but to a lower extent, with, for instance, the integral at (5.50–5.30) ppm decreasing by ~6%. No changes are observed for samples aged under argon atmosphere, whereby these results indicate that both the presence of oxygen and temperature is crucial to the chemical aging process (Figure 4a, all spectra shown in Figure S2).

SEC curves show the main peak for fresh olive oil at ~1300 Da relative to the calibration standard polystyrene. The intensity of a tiny shoulder at ~400 Da increases during aging in the order argon < norm climate < 70 °C. An additional peak appears at ~2600 Da after norm climate aging but not after argon aging, and reaches almost the same intensity as the fresh olive oil peak after aging at 70 °C. An overall widespread content of higher molecular weight fractions is observed for the thermally aged sample, indicating that di-/oligomerization and other intermolecular reactions such as crosslinking lead to molecular weight increase. However, reactions that lead to lower molecular weight fractions occur under all aging conditions (Figure 4b). Note that the values given for SEC-based molecular weights are not absolute due to the use of polystyrene standards and can only be compared relative to each other, which nonetheless allows for qualitative molecular weight evolution assessment.

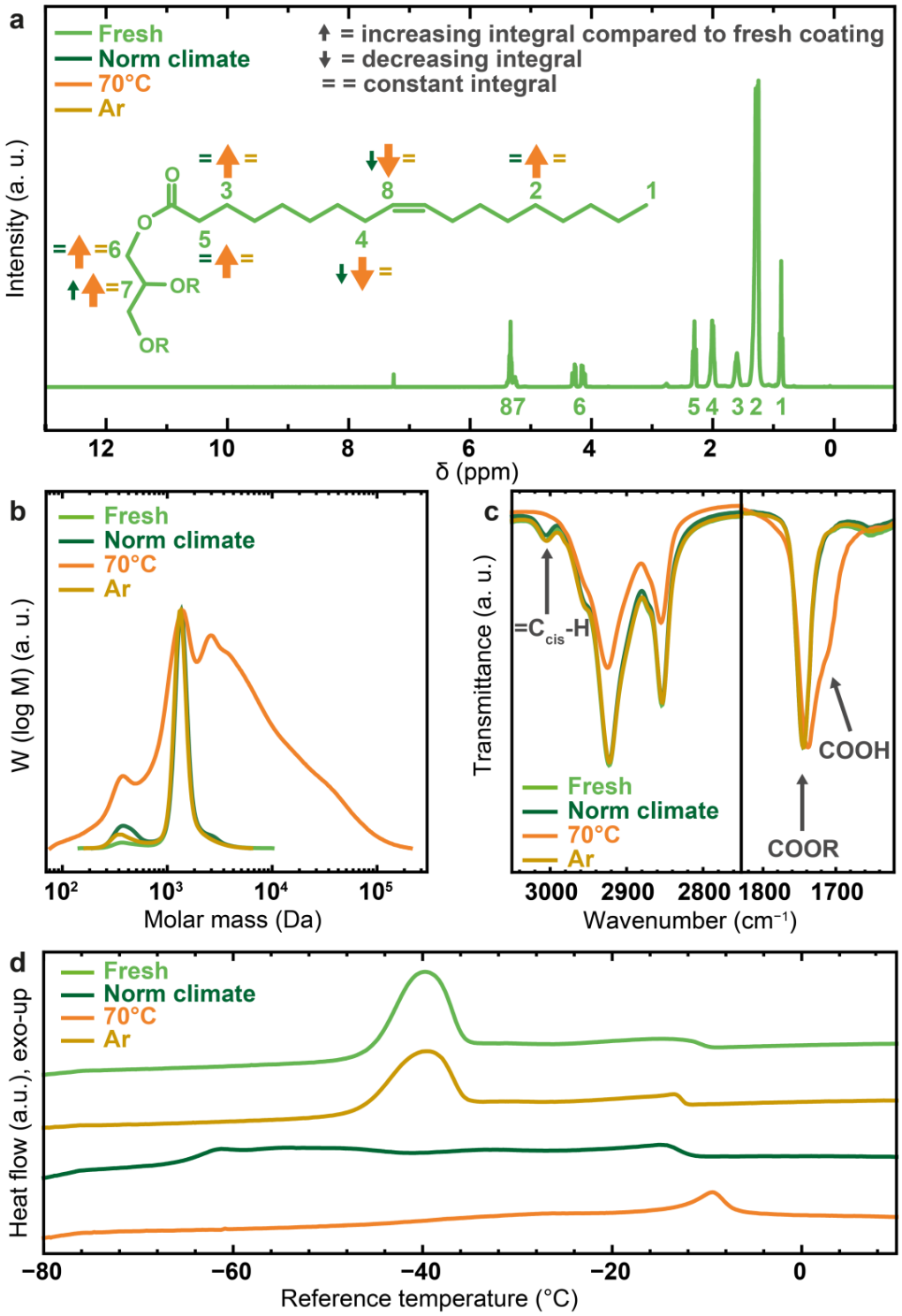

Figure 4. (**a**) ^{1}H-NMR spectrum of olive oil, inset indicating trends after aging for individual hydrogen integrals. (**b**) Normalized SEC curves show the formation of lower molecular weight compounds and of higher molecular weight compounds especially after thermal aging. (**c**) Excerpts of FTIR spectra normalized to C=O peak intensity showing the disappearance of =C_{cis}-H bond in the spectral area from 2775 cm^{-1} to 3025 cm^{-1} and C=O_{acid} shoulder formation in the spectral area from 1625 cm^{-1} to 1825 cm^{-1} after aging at 70 °C. (**d**) DSC cooling curves showing the disappearance of the original triglyceride peak and the emergence of higher and lower molecular weight species. (**a**,**b**) were measured on oil after its extraction from paper; (**c**,**d**) were measured directly on paper, and the results were in accordance with those measured on oil after extraction.

ATR-FTIR spectroscopy highlights interesting properties in the areas of aliphatic and carbonyl vibration bands. While no modifications are observed for the coated samples aged at ambient temperature, the samples aged at 70 °C show several changes. The band indicating $=C_{cis}$-H vibrations at 3005 cm^{-1} disappears completely [36]. The bands at 2956 cm^{-1}, 2923 cm^{-1} and 2853 cm^{-1} can be attributed to asymmetric CH_3 stretching, asymmetric CH_2 stretching and symmetric CH_2 stretching, respectively [36]. Their intensity relative to the carbonyl band at 1745 cm^{-1} is lower for the thermally aged sample, indicating an increased oxygen content relative to the aliphatic chain content. Further, the peak indicating the carbonyl bond shows a slight shift to lower wavenumbers for the coating aged at 70 °C and also features a supplementary shoulder at 1709 cm^{-1}. While the main C=O peak is attributed to the stretching mode of the ester bond present in vegetable oils, the shoulder belongs to the C=O stretching mode of free fatty acids [36], indicating their formation at elevated temperatures as described in the literature (Figure 4c, full spectrum shown in Figure S3) [24,29].

The DSC cooling curve of fresh olive oil shows two exothermic transitions, the first one at ~−14 °C associated with the crystallization of mostly saturated triacylglycerols and the second one at ~−40 °C with the crystallization of unsaturated triacylglycerols [38–40]. Storage under argon atmosphere does not result in significant changes. After storage at norm climate, the crystallization peak of the unsaturated triacylglycerols is not visible anymore, but the crystallization offset is delayed to ~−61 °C. Both hydrolytic degradation and oxidative processes have been described for the auto-oxidation of olive oil at extended storage times, and especially, auto-oxidation can be attributed to the observed extended crystallization range [41,42]. The presence of thus-formed different smaller and larger molecules hinders crystallization, which is reflected in a decreased crystallization enthalpy, which is approximately 48 J/g for the freshly coated oil and decreases to 31 J/g after norm climate and 18 J/g after thermal aging [43]. As for the paper aged at 70 °C, the crystallization enthalpy is still further reduced compared with the other samples, while the crystallization onset shifts to slightly higher temperatures of −10 °C. This shift and the further increased crystallization range can be attributed to additionally enhanced oxidation and resulting coating heterogeneity (Figure 4d) [41].

The different analytical methods allow for drawing conclusions on chemical processes occurring during the storage of olive oil-coated paper. During aging in argon atmosphere, no significant chemical or morphological changes are observed. The slightly increased WCA can therefore be attributed exclusively to the penetration of the coating into the paper during storage. During aging at norm climate, additional small chemical changes happen, for which oxygen accessibility is a prerequisite. These include oxidation reactions discernible in ^{1}H-NMR spectroscopy by an increase in oxygen-adjacent hydrogen peak integral and a decrease in C=C-adjacent hydrogen peak integrals but not visible in less sensitive ATR-FTIR spectroscopy. SEC and DSC also indicate the formation of oxidation products of higher and lower molecular weight than the native olive oil triglyceride that inhibits crystallization. During thermal storage, these effects are strongly intensified and the C=C double bond is nearly fully consumed, as evidenced by both ^{1}H-NMR and ATR-FTIR spectroscopy. A significant amount of native olive oil triglycerides is transformed into lower and higher molecular weight fractions, as reflected in SEC. These factors indicate that in addition to oxidation, crosslinking or dimer-/oligomerization reactions consume the C=C double bond [16,44]. Oxidation products can be intermediate conjugated dienes, peroxides and finally, aldehydes and other low-molecular-weight compounds [18,20]. Furthermore, transesterification reactions are induced by the combination of heat and paper-intrinsic moisture [24,29] that lead to the liberation of free fatty acid evidenced through ATR-FTIR spectroscopy and the covalent attachment of fatty acids onto the hydroxyl groups of cellulose that ultimately results in paper hydrophobization.

To extend the scope of understanding, the coated papers aged at norm climate were examined at different storage times ranging from fresh samples to papers stored for 6 months. The analytical focus was placed on water contact angle measurements to show the effect on

water absorption and on DSC as the strongest indicator for chemical changes. While the initial water contact angle upon droplet deposition does not change significantly with aging time, water absorption speed decreases, initially taking place within less than 10 s and taking more than 3 min after storage for 6 months (Figure 5a). DSC cooling curves reflect the increase in the formation of oxidized species with storage time (Figure 5b). Similar effects were observed for aging at 70 °C for 1 day and 1 week. Water absorption time decreased with storage time and did so much faster than during norm climate aging (Figure 5c). Stable hydrophobization with water contact angles around 130° on the Soxhlet-extracted papers can already be achieved within 1 week of aging (inset Figure 5c), while 1 day proved insufficient for permanent hydrophobization, as droplet absorption was still immediate and water contact angles could not be measured. Similarly, the DSC curve measured after 1 day of storage does not indicate significant chemical modifications, while the DSC curve after 1 week looks very similar to that obtained after 4 weeks (Figure 5d), indicating that the hydrophobization process can be further tuned by time and temperature. Thus, not only storage conditions but also storage time can have a crucial influence on the physical and chemical properties of vegetable oil-based paper coatings.

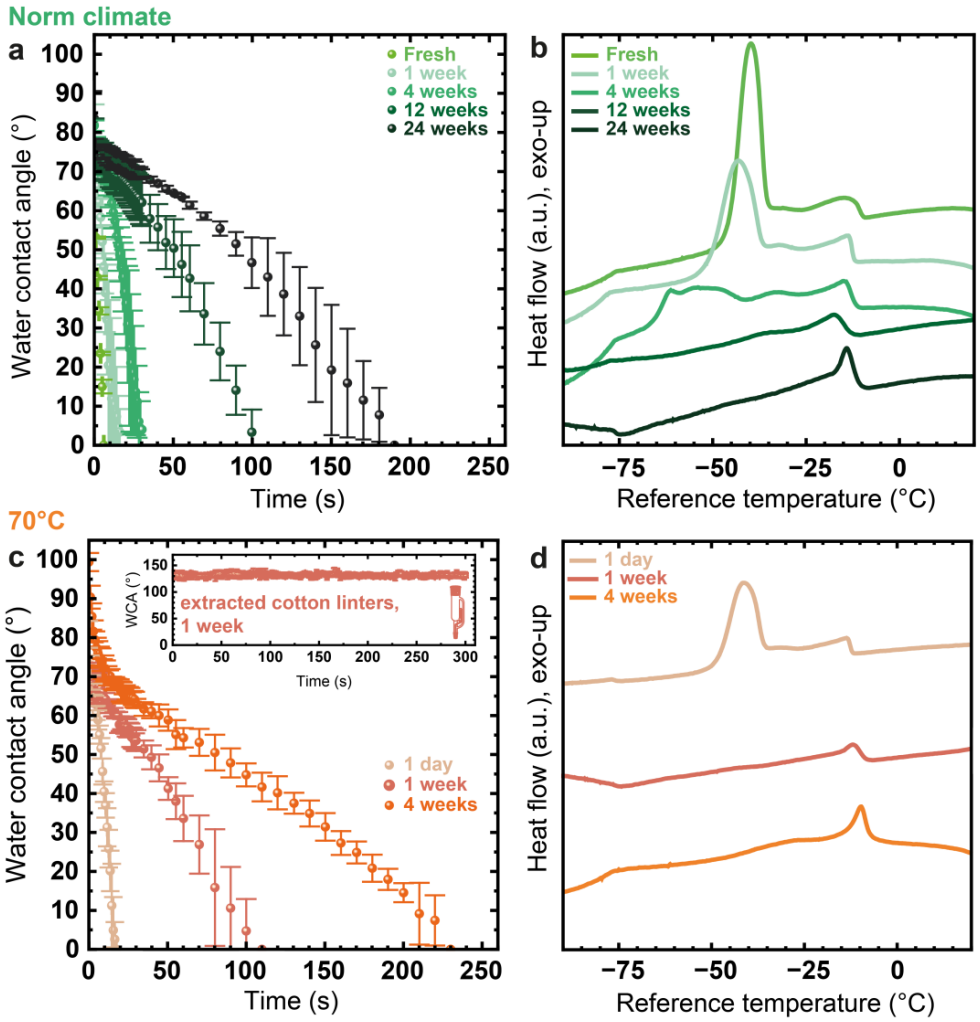

Figure 5. (**a**) Time-dependent WCA measurements show decreasing water absorbance speed with norm climate aging. (**b**) DSC cooling curves show the disappearance of the original triglyceride solidification peak and the occurrence of lower and higher molecular weight species with increasing aging time at norm climate. (**c**) Time-dependent WCA measurements showing absorption after varying aging times at 70 °C and (c-inset) on Soxhlet-extracted paper aged for 1 week. (**d**) DSC measurements indicate significant chemical modification even after 1 week of storage.

4. Conclusions and Outlook

In this work, we have shown that it is possible to produce olive oil-based paper coatings with water contact angles of more than 135° through a 4-week thermal treatment process followed by extraction of unbound vegetable oil, leaving behind an extremely low amount of coating attached covalently to the paper substrate. While this actual procedure is surely not immediately relevant for industrial application, it shows the potential to produce biobased hydrophobic coatings in an extraordinarily simple manner. Choosing a less material-consuming coating method, such as spray coating or gas-phase deposition, would be required to forego the extraction process, while careful tuning of treatment temperature and moisture exposition could greatly accelerate the covalent attachment process. Inquiries into both the recyclability of the coated papers as well as the reusability of the extracted oil are equally relevant for potential industrial applications. Analyzing the modifications occurring both during the thermal aging process and during the practically relevant storage at ambient conditions has proven the cruciality of storage time, temperature and oxygen accessibility for the properties of fatty acid-based coatings. Research in the field of fatty acid-based paper coatings must therefore consider these factors to allow for the reproducibility of results and to be able to account for the long-term stability of the coating.

Supplementary Materials: The following supporting information can be downloaded at: https://www.mdpi.com/article/10.3390/coatings14030364/s1, Protocol for gas chromatography–mass spectrometry/flame ionization detector (GC-MS/FID); Figure S1: Full ATR-FTIR spectrum of extracted cotton linters after varying aging processes showing a small C=O band indicating esterification exclusively after thermal aging; Figure S2: Full NMR spectra of olive oil extracted from cotton linters (fresh and after aging); Figure S3: ATR-FTIR spectra normalized to C=O peak intensity of freshly olive oil coated cotton linter paper and aged under different conditions.

Author Contributions: Conceptualization, A.L.-Z. and A.G.; investigation, A.L.-Z. and T.M.; writing—original draft preparation, A.L.-Z.; writing—review and editing, all authors; visualization, A.L.-Z.; supervision, A.G. and M.B. All authors have read and agreed to the published version of the manuscript.

Funding: This research was funded as part of the BioPlas4Paper project by the Agency for Renewable Resources (Fachagentur Nachwachsende Rohstoffe e.V.—FNR), grant number 2220HV017A.

Institutional Review Board Statement: Not applicable.

Informed Consent Statement: Not applicable.

Data Availability Statement: The data presented in this study are available on request from the corresponding authors.

Acknowledgments: The authors thank Marion Trautmann for SEC measurements and the NMR service group (all Department of Chemistry, Technical University Darmstadt) for service NMR measurements as well as Silke Radtke (Thünen Institute for Wood Research, Hamburg) for GC-MS/FID measurements.

Conflicts of Interest: The authors declare no conflicts of interest.

References

1. Samyn, P. Active Barrier Coating for Packaging Paper with Controlled Release of Sunflower Oils. *Molecules* **2021**, *26*, 3561. [CrossRef] [PubMed]
2. Crépy, L.; Chaveriat, L.; Banoub, J.; Martin, P.; Joly, N. Synthesis of cellulose fatty esters as plastics—Influence of the degree of substitution and the fatty chain length on mechanical properties. *ChemSusChem* **2009**, *2*, 165–170. [CrossRef] [PubMed]
3. David, G.; Gontard, N.; Guerin, D.; Heux, L.; Lecomte, J.; Molina-Boisseau, S.; Angellier-Coussy, H. Exploring the potential of gas-phase esterification to hydrophobize the surface of micrometric cellulose particles. *Eur. Pol. J.* **2019**, *115*, 138–146. [CrossRef]
4. Peydecastaing, J.; Girardeau, S.; Vaca-Garcia, C.; Borredon, M.E. Long chain cellulose esters with very low DS obtained with non-acidic catalysts. *Cellulose* **2006**, *13*, 95–103. [CrossRef]
5. Geissler, A.; Loyal, F.; Biesalski, M.; Zhang, K. Thermo-responsive superhydrophobic paper using nanostructured cellulose stearoyl ester. *Cellulose* **2014**, *21*, 357–366. [CrossRef]
6. Nau, M.; Seelinger, D.; Biesalski, M. Functional surface coatings from tailor-made long-chain hydroxypropyl cellulose ester nanoparticles. *Cellulose* **2018**, *25*, 5769–5780. [CrossRef]

7. Cordt, C.; Geissler, A.; Biesalski, M. Regenerative Superhydrophobic Paper Coatings by In Situ Formation of Waxy Nanostructures. *Adv. Mater. Interfaces* **2021**, *8*, 2001265. [CrossRef]
8. Onwukamike, K.N.; Grelier, S.; Grau, E.; Cramail, H.; Meier, M.A.R. Sustainable transesterification of cellulose with high oleic sunflower oil in a DBU-CO2 switchable solvent. *ACS Sustain. Chem. Eng.* **2018**, *6*, 8826–8835. [CrossRef]
9. Huang, X.; Wang, A.; Xu, X.; Liu, H.; Shang, S. Enhancement of hydrophobic properties of cellulose fibers via grafting with polymeric epoxidized soybean oil. *ACS Sustain. Chem. Eng.* **2017**, *5*, 1619–1627. [CrossRef]
10. Saha, P.; Manna, S.; Sen, R.; Roy, D.; Adhikari, B. Durability of lignocellulosic fibers treated with vegetable oil–phenolic resin. *Carbohydr. Polym.* **2012**, *87*, 1628–1636. [CrossRef]
11. Shang, Q.; Liu, C.; Chen, J.; Yang, X.; Hu, Y.; Hu, L.; Zhou, Y.; Ren, X. Sustainable and robust superhydrophobic cotton fabrics coated with castor oil-based nanocomposites for effective oil–water separation. *ACS Sustain. Chem. Eng.* **2020**, *8*, 7423–7435. [CrossRef]
12. Loesch-Zhang, A.; Cordt, C.; Geissler, A.; Biesalski, M. A Solvent-Free Approach to Crosslinked Hydrophobic Polymeric Coatings on Paper Using Vegetable Oil. *Polymers* **2022**, *14*, 1773. [CrossRef] [PubMed]
13. Bellmann, M.; Loesch-Zhang, A.; Möck, D.M.J.; Appelt, J.; Geissler, A.; Viöl, W. Hydrophobic glass and paper coatings based on plasma polymerized vegetable oils using a novel atmospheric pressure plasma concept. *Plasma Process. Polym.* **2024**, e202300224. [CrossRef]
14. Samyn, P. Wetting and hydrophobic modification of cellulose surfaces for paper applications. *J. Mater. Sci.* **2013**, *48*, 6455–6498. [CrossRef]
15. Dankovich, T.A.; Hsieh, Y.-L. Surface modification of cellulose with plant triglycerides for hydrophobicity. *Cellulose* **2007**, *14*, 469–480. [CrossRef]
16. Bilancia, M.T.; Caponio, F.; Sikorska, E.; Pasqualone, A.; Summo, C. Correlation of triacylglycerol oligopolymers and oxidised triacylglycerols to quality parameters in extra virgin olive oil during storage. *Food Res. Int.* **2007**, *40*, 855–861. [CrossRef]
17. Kanavouras, A.; Cert, A.; Hernandez, R.J. Oxidation of Olive Oil under Still Air. *Food Sci. Technol. Int.* **2005**, *11*, 183–189. [CrossRef]
18. Gómez-Alonso, S.; Salvador, M.D.; Fregapane, G. Evolution of the oxidation process in olive oil triacylglycerol under accelerated storage conditions (40–60 °C). *J. Am. Oil Chem. Soc.* **2004**, *81*, 177–184. [CrossRef]
19. Ixtaina, V.Y.; Nolasco, S.M.; Tomás, M.C. Oxidative Stability of Chia (*Salvia hispanica* L.) Seed Oil: Effect of Antioxidants and Storage Conditions. *J. Am. Oil Chem. Soc.* **2012**, *89*, 1077–1090. [CrossRef]
20. Guiotto, E.N.; Ixtaina, V.Y.; Nolasco, S.M.; Tomás, M.C. Effect of Storage Conditions and Antioxidants on the Oxidative Stability of Sunflower–Chia Oil Blends. *J. Am. Oil Chem. Soc.* **2014**, *91*, 767–776. [CrossRef]
21. Malvis, A.; Šimon, P.; Dubaj, T.; Sládková, A.; Ház, A.; Jablonský, M.; Sekretár, S.; Schmidt, Š.; Kreps, F.; Burčová, Z.; et al. Determination of the Thermal Oxidation Stability and the Kinetic Parameters of Commercial Extra Virgin Olive Oils from Different Varieties. *J. Chem.* **2019**, *2019*, 4567973. [CrossRef]
22. van Durme, J.; Nikiforov, A.; Vandamme, J.; Leys, C.; de Winne, A. Accelerated lipid oxidation using non-thermal plasma technology: Evaluation of volatile compounds. *Food Res. Int.* **2014**, *62*, 868–876. [CrossRef]
23. Tenbohlen, S.; Koch, M. Aging Performance and Moisture Solubility of Vegetable Oils for Power Transformers. *IEEE Trans. Power Deliv.* **2010**, *25*, 825–830. [CrossRef]
24. Bandara, K.; Ekanayake, C.; Saha, T.K.; Annamalai, P.K. Understanding the ageing aspects of natural ester based insulation liquid in power transformer. *IEEE Trans. Dielect. Electr. Insul.* **2016**, *23*, 246–257. [CrossRef]
25. Rooney, D.; Weatherley, L.R. The effect of reaction conditions upon lipase catalysed hydrolysis of high oleate sunflower oil in a stirred liquid–liquid reactor. *Process Biochem.* **2001**, *36*, 947–953. [CrossRef]
26. Zervos, S. Natural and accelerated ageing of cellulose and paper: A literature review. In *Cellulose: Structure and Properties, Derivatives and Industrial Uses*; Lejeune, A., Deprez, T., Eds.; Nova Science Publishers: Hauppauge, NY, USA, 2010; ISBN 9781608763887.
27. Contreras, J.E.; Rodriguez, J.; Gaytan, C.; Greaves, B.; Prevost, T. Thermal Aging Performance of Cellulose Insulation in Natural Ester Liquid. *IEEE Trans. Dielect. Electr. Insul.* **2021**, *28*, 1357–1362. [CrossRef]
28. Franquet, J.; Fernandez, I.; Ortiz, A. Dielectric and Mechanical Assessment of Kraft and Diamond Dotted Paper Aged with Commercial Vegetable Oil. In Proceedings of the 2020 IEEE International Conference on Dielectrics. 2020 IEEE 3rd International Conference on Dielectrics (ICD), Valencia, Spain, 5–31 July 2020; pp. 696–699, ISBN 978-1-7281-8983-3.
29. Rapp, K.J.; McShane, C.P.; Luksich, J. Interaction mechanisms of natural ester dielectric fluid and kraft paper. In Proceedings of the 2005 IEEE International Conference on Dielectric Liquids. ICDL 2005, Coimbra, Portugal, 26 June–1 July 2005; pp. 387–390, ISBN 0-7803-8954-9.
30. Nguyen, D.V.; Nguyen, L.P.; Quach, T.N. Investigation of AC breakdown properties of paper insulators and enamel insulation impregnated with rice oil, corn oil and peanut oil for transformers. *IET Sci. Meas.* **2019**, *13*, 1352–1361. [CrossRef]
31. McShane, C.P.; Gauger, G.A.; Luksich, J. Fire resistant natural ester dielectric fluid and novel insulation system for its use. In Proceedings of the IEEE Transmission and Distributions Conference (Cat. No. 99CH36333), New Orleans, LA, USA, 11–16 April 1999; pp. 890–894.
32. Yang, L.; Liao, R.; Caixin, S.; Zhu, M. Influence of vegetable oil on the thermal aging of transformer paper and its mechanism. *IEEE Trans. Dielect. Electr. Insul.* **2011**, *18*, 692–700. [CrossRef]
33. *ISO 5269-2:2004(E)*; Pulps—Preparation of Laboratory Sheets for Physical Testing—Part 2: Rapid-Köthen Method. International Organization for Standardization: Geneva, Switzerland, 2004.

34. Rueden, C.T.; Schindelin, J.; Hiner, M.C.; DeZonia, B.E.; Walter, A.E.; Arena, E.T.; Eliceiri, K.W. ImageJ2: ImageJ for the next generation of scientific image data. *BMC Bioinform.* **2017**, *18*, 529. [CrossRef]
35. *ISO 25178-2:2021(E)*; Geometrical Product Specifications (GPS)—Surface Texture: Areal—Part 2: Terms, Definitions and Surface Texture Parameters. International Organization for Standardization: Geneva, Switzerland, 2021.
36. Zhang, Q.; Liu, C.; Sun, Z.; Hu, X.; Shen, Q.; Wu, J. Authentication of edible vegetable oils adulterated with used frying oil by fourier transform infrared spectroscopy. *Food Chem.* **2012**, *132*, 1607–1613. [CrossRef]
37. Sacchi, R.; Addeo, F.; Paolillo, L. 1H and 13C NMR of virgin olive oil. An overview. *Magn. Reson. Chem.* **1997**, *35*, 133–145. [CrossRef]
38. Chiavaro, E.; Vittadini, E.; Rodriguez-Estrada, M.T.; Cerretani, L.; Bonoli, M.; Bendini, A.; Lercker, G. Monovarietal extra virgin olive oils: Correlation between thermal properties and chemical composition. *J. Agric. Food Chem.* **2007**, *55*, 10779–10786. [CrossRef] [PubMed]
39. Barba, L.; Arrighetti, G.; Calligaris, S. Crystallization and melting properties of extra virgin olive oil studied by synchrotron XRD and DSC. *Eur. J. Lipid Sci. Technol.* **2013**, *115*, 322–329. [CrossRef]
40. Che Man, Y.B.; Tan, C.P. Comparative differential scanning calorimetric analysis of vegetable oils: II. Effects of cooling rate variation. *Phytochem. Anal.* **2002**, *13*, 142–151. [CrossRef] [PubMed]
41. Chiavaro, E.; Mahesar, S.A.; Bendini, A.; Foroni, E.; Valli, E.; Cerretani, L. DSC Evaluation of Olive Oil during Accelerated Oxidation. *Ital. J. Food Sci.* **2011**, *23*, 164–172.
42. Chiavaro, E.; Cerretani, L.; Paradiso, V.M.; Summo, C.; Paciulli, M.; Gallina Toschi, T.; Caponio, F. Thermal and chemical evaluation of naturally auto-oxidised virgin olive oils: A correlation study. *J. Sci. Food Agric.* **2013**, *93*, 2909–2916. [CrossRef] [PubMed]
43. Vittadini, E.; Lee, J.H.; Frega, N.G.; Min, D.B.; Vodovotz, Y. DSC determination of thermally oxidized olive oil. *J. Am. Oil Chem. Soc.* **2003**, *80*, 533–537. [CrossRef]
44. Dobarganes, M.C.; Pérez-Camino, M.C.; Márquez-Ruíz, G. High Performance Size Exclusion Chromatography of Polar Compounds in Heated and Non-Heated Fats. *Fat. Sci. Technol.* **1988**, *90*, 308–311. [CrossRef]